Appl Phys A (2014) 114:1209–1213
DOI 10.1007/s00339-013-7845-6

Applied Physics A
Materials Science & Processing

Synthesis of ZnO nanowires on aluminum flake by aqueous method

Naisen Yu · Haifeng Zhao · Ligong Zhang · Danyang Hu · Xueying Ma · Bin Dong

Received: 20 March 2013 / Accepted: 4 July 2013 / Published online: 6 August 2013

Abstract ZnO nanowires are grown on aluminum flake at low temperature by using a simple aqueous solution method. X-Ray Diffraction (XRD), Scanning Electron Microscopy (SEM) and Transmission Electron Microscope (TEM) are applied to determine the as-grown ZnO nanowires morphology and crystal structures. The results show that the ZnO nanowires have wurtzite structure, and the diameter and length of the nanowire are 30 nm and more than 1.5 μm, respectively. Photoluminescence spectroscopy (PL) and Raman spectrum reveal the nanowires have good optical properties with low tensile stress. Meanwhile, photoelectrochemical cell (PEC) study verifies that ZnO nanowires as photoanodes are relatively stable in the photo-oxidation process, which could be a promising technique for practical applications.

1 Introduction

With a direct wideband gap (3.37 eV) and a large exciton binding energy (60 meV), ZnO is recognized as a promising optoelectronic material in the blue-ultraviolet UV region and an excellent candidate for a dye-sensitized oxide semiconductor solar cell [1–3]. It is predicted that the gas sensing, photon-to-electron conversion efficiency and photonic performance would be enhanced by reducing the dimensions. Therefore, considerable efforts are devoted to explore effective methods to synthesize ZnO with tunable size and morphology [4]. Various synthesis routes, such as thermal evaporation, chemical vapor deposition, carbon-thermal reduction, low-temperature oxidization, template-assisted growth, and solution-based approaches, have been developed to synthesize ZnO with various morphologies [5–8]. However, most of the synthesis techniques demand vacuum, high temperature, or complicated controlling processes, which are unfavorable for low-cost and large-scale production. Therefore, it is of great importance and necessity to develop a technique to synthesize ZnO in mild reaction conditions. Solution chemical routes have been proven to be a versatile approach for preparation of ZnO due to the convenience and simplicity [9, 10]. But up to now, growth of nanowires with large length has not been achieved by aqueous solution method. The diameter of ZnO nanocrystals is dependent on the concentration of the solution [11, 12], nanorods can be obtained when the concentration is relatively low, but nanowires cannot, because the concentration of the solution will decrease greatly with the crystal growth. So, to get nanowires with larger length, it is essential to maintain the concentration of the solution during the whole growth process [13].

In this paper, we report the preparation of ZnO nanowires grown on aluminum flake in aqueous method. By adding NaF, controllable ZnO nanowires can be obtained. The as-grown ZnO nanowires are characterized using X-ray diffraction (XRD), field emission scanning electron microscopy (FESEM), transmission electron microscopy (TEM), Raman spectroscopy and photoluminescence spectroscopy (PL). The XRD studies reveal that the ZnO nanowires

N. Yu (✉) · D. Hu · X. Ma · B. Dong
Institute of Optoelectronic Technology, School of Physics and Materials Engineering, Dalian Nationalities University, Dalian 116600, China
e-mail: yunaisen@gmail.com
Fax: +86-411-87656135

H. Zhao · L. Zhang
State Key Laboratory of Luminescence and Applications, Changchun Institute of Optics, Fine Mechanics and Physics, Chinese Academy of Sciences, 130033 Changchun, Jilin, China

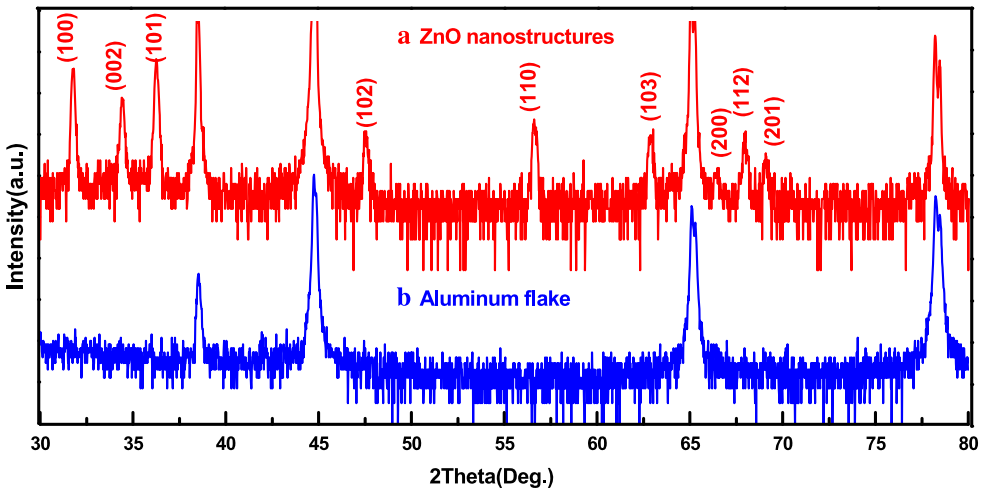

Fig. 1 X-ray diffraction patterns of ZnO nanowires: (**a**) aluminum flake; (**b**) ZnO nanowires grown on aluminum flake

have wurtzite structure. The microscopic studies show that the diameter and length of the nanowire are 30 nm and more than 1.5 μm, respectively. Optical characterization shows that nanowires have good optical properties with low tensile stress. Meanwhile, amperometric I–t result verifies that photogenerated electrons are rapidly transported from ZnO nanowires, which could be used as a promising technique for practical applications.

2 Experimental design

The ZnO nanostructures were grown on aluminum flake by a two-step method, including the synthesis of homo-seed layer and the growth of ZnO nanostructures in aqueous solutions at low temperature. The aluminum flake was seeded via spin-coating by 0.02 M zinc acetate ($Zn(CH_3COO)_2 \cdot 2H_2O$) solution. Then the aluminum flake was annealed at 200 °C to achieve a good adhesion between the seeding layer and substrate. The typical procedure for the preparation of ZnO nanowires was as follows: an equimolar (0.05 M) aqueous solution of zinc nitrate ($Zn(NO_3)_2$) and hexamethyltetramine ($C_6H_{12}N_4$) was dissolved in distilled water and the solution was stirred at room temperature. Then 0.02 M NaF was added under stirring condition. The seeded aluminum flake was put into the above solution of 90 °C for 5 h. After deposition, the samples were cleaned with de-ionized water and then dried in an air atmosphere. Meanwhile, an equimolar (0.05 M) aqueous solution of zinc nitrate ($Zn(NO_3)_2$) and hexamethyltetramine ($C_6H_{12}N_4$) without NaF was also applied on the seeded aluminum flake for reference. All the chemical reagents were of analytical grade and used without further purification. After deposition, the samples were cleaned with de-ionized water and then dried in an air atmosphere.

3 Results and discussion

The structural properties of as-grown ZnO nanowires were characterized by X-ray diffraction (XRD). The morphology of the as-prepared nanowires was observed using Hitachi S-4800 field-emission scanning electron microscopy (FE-SEM). TEM characterization was performed by JEM-2000EX. And optical properties were studied by PL and Raman spectra. The PL spectrum was measured at room temperature with a He–Cd laser. Both the Raman and PL measurements were performed at room temperature. Raman spectrum was measured with confocal Raman spectroscopic system (Renishaw2000, Invia). The 632.8-nm radiation from the He–Ne laser was used as an exciting source. Electrochemical experiments were characterized by using a Princeton Applied Research PARSTAT 2263 advanced electrochemical analyzer. The electrochemical measurement was executed in a standard three-electrode system at room temperature.

Figure 1 illustrates the typical X-ray diffraction patterns of the ZnO nanowires and aluminum flake. The positions and relative intensities of the diffraction peaks are in good agreement with the Powder Diffraction Standards data (JCPDS No. 076-0704). And it shows that the main structure of the samples is the wurtzite structure of ZnO. No peaks corresponding to NaF crystals or other phases are detected for the sample with NaF adding. Moreover, the X-ray diffraction pattern shows narrow and sharp diffraction peaks which indicate good crystallinity of the sample.

Typical SEM images of as-grown ZnO nanostructures grown on aluminum flake without and with NaF addition are shown in Fig. 2. Figure 2(a) shows low-magnification SEM images of ZnO nanostructures grown on aluminum flake without NaF addition. It can be clearly seen that film-like structure is synthesized on aluminum flake. According to the careful examination from the enlarged image in Fig. 2(b),

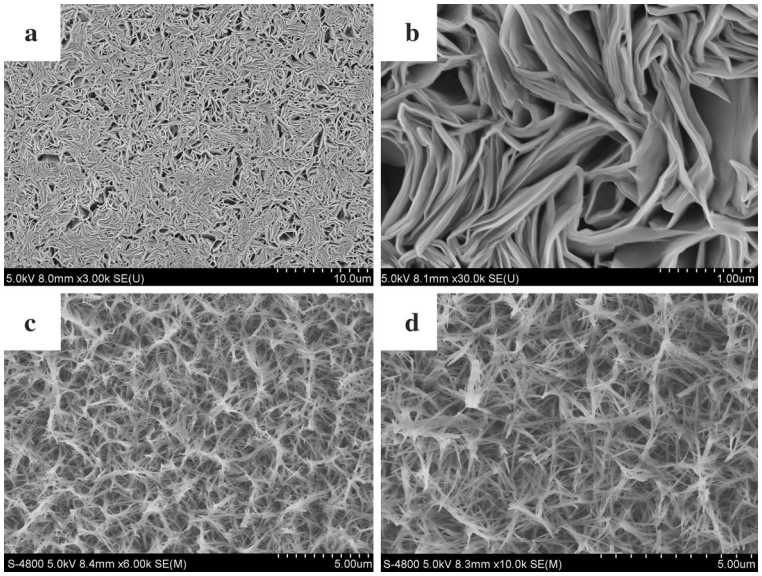

Fig. 2 Typical SEM images of ZnO nanostructures grown on aluminum flake without and with NaF addition. (**a**), (**b**): Low- and high-magnification FE-SEM of ZnO nanostructures grown on aluminum flake; (**c**), (**d**): Low- and high-magnification FE-SEM of ZnO nanostructures grown on aluminum flake with NaF addition

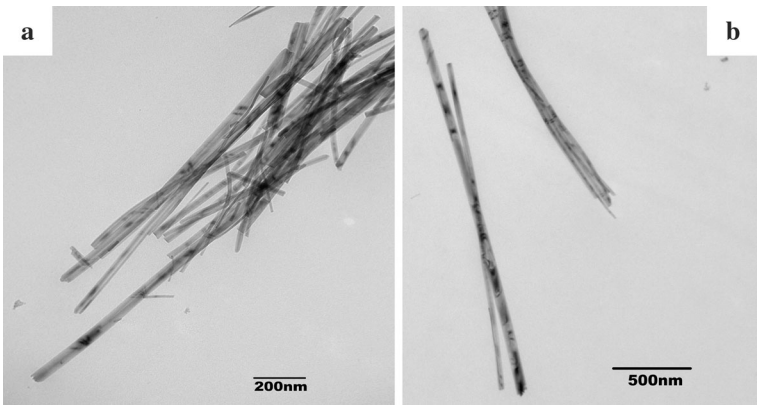

Fig. 3 Typical TEM images of ZnO nanowire grown on aluminum flake

the film is composed of a large amount of ribbon-like nanostructures with their planes predominantly perpendicular to the substrate. And the ribbon-like structures exhibit curved anomalous morphology. These dense ribbon-like nanostructures were dispersed quasi-vertically and homogeneously on aluminum substrates. Typical SEM images of as-grown ZnO nanowires with NaF adding are shown in Fig. 2. The low-magnified of as-grown sample is shown in Fig. 2(c). The SEM image indicates that the structures consist of dense and vertically aligned ZnO nanowires. Figure 2(d) shows the high magnified view of the SEM image: it can be clearly seen that the oriented nanowires are dispersively distributed on the aluminum flake. Meanwhile, the nanowires typically connect with the neighboring structures, resulting in free-standing wire clusters.

For the TEM study, the samples were made by removing the nanostructures from the aluminum substrate by scratching, and then dispersing in ethanol, followed by sonication for 10 min. The ethanol solution was spread on a few copper grids. Figure 3 shows the TEM image of the typical ZnO nanowires. Large quantities of uniform wire-like nanostructures are observed. The diameter of the nanowire is about 30 nm with length more than 1.5 μm.

The growth mechanism of nanowires structures can be attributed to the NaF addition. In general, the growth of ZnO crystals is controlled by nucleation and growth processes in aqueous solution. And the chemical reaction processes by using $Zn(NO_3)_2$ and $C_6H_{12}N_4$ as the precursors can be described as follows:

$$(CH_2)_6N_4 + 6H_2O \rightarrow 6HCHO + 4NH_3 \quad (1)$$

$$NH_3 + H_2O \rightarrow NH_4^+ + OH^- \quad (2)$$

$$2OH^- + Zn^{2+} \rightarrow Zn(OH)_2 \quad (3)$$

$$Zn(OH)_2 \rightarrow ZnO + H_2O \quad (4)$$

In our case, the aluminum flake with ZnO seeding layer will provide the nucleation sites and promote ZnO nanostructures growth. Under the NaF doping reaction system, the Na^+ cations, with a small radius, lead to a weak influence on the prior growth orientation of ZnO nanocrystal along the *c*-axis, whereas the F^- cations will react with the Zn^{2+} to

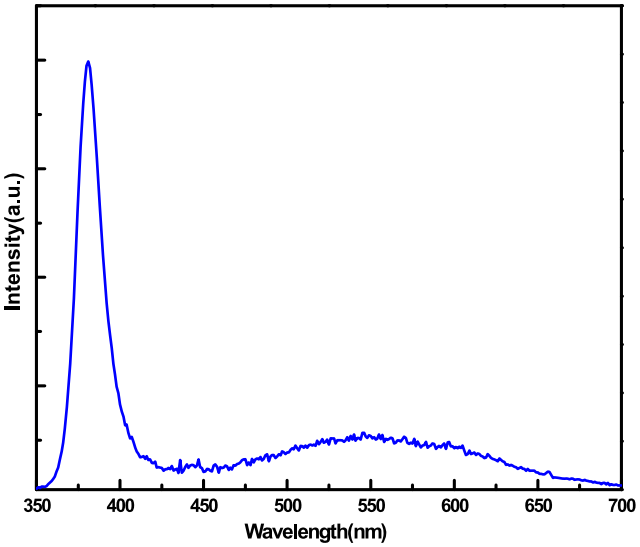

Fig. 4 Room-temperature PL spectra of ZnO nanowire grown on aluminum flake

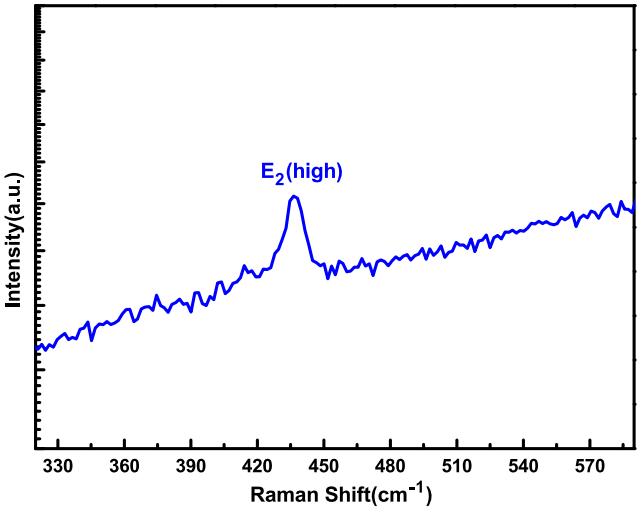

Fig. 5 Room-temperature Raman spectra of ZnO nanowire grown on aluminum flake

form ZnOHF and lead to the lower precursor concentration. The reaction can be described as follows:

$$Zn^{2+} + F^- \rightarrow ZnF^+ \quad (5)$$

$$NO_3^- + H_2O + 2e^- \rightarrow NO_2^- + 2OH^- \quad (6)$$

$$ZnF^+ + OH^- \rightarrow ZnOHF \quad (7)$$

In addition, due to the strong coordination of the most electronegative F^- anions to Zn^+ cations, the nanostructures can be decomposed into axial and radial directions, respectively [14]. Thus, ZnO nanowires structures can be achieved by adopting NaF in the $Zn(NO_3)_2$ and $C_6H_{12}N_4$ reaction system.

The optical properties of the ZnO nanostructures were studied by means of room-temperature PL measurement. The typical PL spectrum is shown in Fig. 4. The PL spectrum is characterized by two emissions, a strong and dominant sharp peak around 380 nm, and a weak and broad peak centered around 550 nm. The peak observed at around 380 nm in the UV region is due to free exciton emissions, that is, near band-edge emission. While the weak, broad peak in the visible region is attributed to deep level emissions. It has been suggested that the green band emission corresponds to the singly ionized oxygen vacancy in ZnO [15–18]. In general, comparing the ratio of the relative PL intensity of the excitonic emission to the visible emission (I_{uv}/I_{vis}) is a way to evaluate the quality of the ZnO structures [19]. The ratio of peak intensities of I_{uv}/I_{vis} in the PL spectra of the nanostructures is 7.2. Therefore, the PL results indicate that the ZnO nanostructures have good crystal quality and low concentration of defects.

Figure 5 presents a typical micro-Raman spectrum of ZnO nanostructures. It was taken in the backscattering configuration at room temperature. According to the selection rule of the photon mode in hexagonal wurtzite-structure ZnO, the peak at 436.7 cm^{-1} is assigned to the high frequency E_2 (high) mode. Huang et al. have demonstrated that the stress induced in crystal would obviously affect the E_2 (high) phonon frequency [20]. An increase in the E_2 (high) photon frequency was ascribed to compressive stress, whereas a decrease in the E_2 (high) photon frequency was ascribed to tensile stress. For the ZnO nanostructures grown on aluminum flake, the E_2 (high) mode is at 436.7 cm^{-1}, which downshifts in comparison with the stress-free bulk ZnO value of 437 cm^{-1} [21], indicating that the ZnO nanostructures suffer from a tensile stress. The correlation between the Raman shift and the stress can be simply expressed as $\Delta\omega\ (cm^{-1}) = 4.4\sigma$ (GPa) [21]. According to this formula, the tensile stress of ZnO nanostructures is 0.07 GPa. Thus, the ZnO nanostructures on aluminum flake are under lower tensile stress.

The photoelectrochemical cell (PEC) study was carried out in 0.5 M Na_2SO_4 (pH 7.0) solution, which served as supporting electrolyte medium. Amperometric I–t curve of ZnO nanowires was obtained at an applied voltage of +0.5 V. Figure 6 plots the amperometric I–t curves of ZnO nanowires with on/off cycles. Upon illumination, a spike in the photoresponse can be observed. It is due to the transient effect in power excitation before the photocurrent quickly returned to a steady state. This result verifies that photogenerated electrons are rapidly transported from ZnO nanowires. Importantly, we only observe a small decay of photocurrent density in a continuous running, which indicates that the ZnO nanowires as photoanodes are relatively stable in the photo-oxidation process.

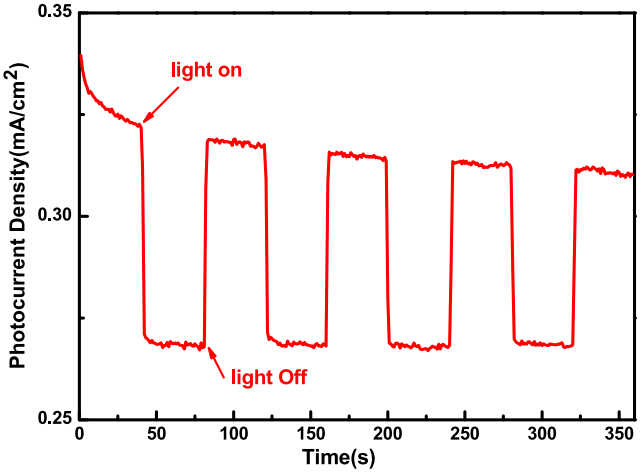

Fig. 6 Amperometric I–t curves of t ZnO nanowires at 100 mW/cm^2 with on/off cycles

4 Conclusion

In summary, the single-crystalline ZnO nanowires were successfully prepared on aluminum substrate by the aqueous method at relative low temperature. By adding NaF, controllable ZnO nanowires with wurtzite structure were obtained. Optical characterization showed that ZnO nanowires had good optical properties with low tensile stress. Meanwhile, amperometric I–t result verified that photogenerated electrons were rapidly transported from ZnO nanowires, which could be used as a promising technique for practical applications.

Acknowledgements This work was supported by the National Natural Science Foundation of China (Grant No. 51102036), Fundamental Research Funds for the Central Universities DC12010207, Program for Liaoning Excellent Talents in University (No. LJQ2012116) and Dalian Science and Technology Funding project (No. 2012J21DW015).

References

1. Y. Huang, X.F. Duan, Y. Cui, L.J. Lauhon, K.H. Kim, C.M. Lieber, Science **294**, 1313 (2001)
2. A.B.F. Martinson, J.W. Elam, J.T. Hupp, M.J. Pellin, Nano Lett. **7**, 2183 (2007)
3. T.B. Hur, Y.H. Hwang, H.K. Kim, J. Appl. Phys. **96**, 1507 (2004)
4. H.M. Chen, Y.F. Chen, M.C. Lee, M.S. Feng, Phys. Rev. B **56**, 6942 (1997)
5. B. Lin, Z. Fu, Appl. Phys. Lett. **79**, 943 (2001)
6. K. Govender, D.S. Boyle, O.P. Brien, D. Bink, D. West, D. Coleman, Adv. Mater. **14**, 1221 (2002)
7. J.J. Wu, S.C. Liu, C.T. Wu, K.H. Chen, C.L. Chen, Appl. Phys. Lett. **81**, 1312 (2002)
8. A. Pan, R. Yu, S. Xie, Z. Zhang, C. Jin, B. Zou, J. Cryst. Growth **28**, 2165 (2005)
9. W.I. Park, D.H. Kim, S.W. Jung, G.C. Yi, Appl. Phys. Lett. **80**, 4232 (2002)
10. S. Kar, B.N. Pal, S. Chaudhuri, D. Chakravorty, J. Phys. Chem. B **110**, 4605 (2006)
11. L. Vayssieres, Adv. Mater. **15**, 464 (2003)
12. X. Liu, Z. Jin, S. Bu, J. Zhao, Z. Liu, J. Am. Ceram. Soc. **89**, 1226 (2006)
13. S.J. Bu, C.X. Cui, Q.Z. Wang, L. Bai, J. Nanomater. **2008**, 610541 (2008)
14. G.Y. Zhang, X.D. Bai, E.G. Wang, Phys. Rev. B **71**, 113411 (2005)
15. T. Fukumura, Z.W. Jin, M. Kawasaki, T. Shono, T. Hasegawa, S. Koshihara, H. Koinuma, Appl. Phys. Lett. **78**, 958 (2001)
16. V. Srikant, D.R. Clarke, J. Appl. Phys. **83**, 5447 (1998)
17. S.Y. Ma, X.H. Yang, X.L. Huang, A.M. Sun, H.S. Song, H.B. Zhu, J. Alloys Compd. **566**, 9 (2013)
18. M. Yang, G.F. Yin, Z.B. Huang, Y.Q. Kang, X.M. Liao, H. Wang, Cryst. Growth Des. **9**, 707 (2009)
19. F. Xu, Y.N. Lu, L.T. Sun, L.J. Zhi, Chem. Commun. **46**, 3191 (2010)
20. Y. Huang, M. Liu, Z. Li, Y. Zeng, S. Liu, Mater. Sci. Eng. B **97**, 111 (2003)
21. F. Decremps, J.P. Porres, A.M. Saitta, J.C. Chervin, A. Polian, Phys. Rev. B **65**, 109210 (2002)